



Dimethylamine formation from N-nitrosodimethylamine adsorbed on the Ni{1 1 1} surface from first principles

Víctor A. Ranea

CCT-La Plata-CONICET, Instituto de Investigaciones Físico-químicas Teóricas y Aplicadas (INIFTA), Facultad de Ciencias Exactas, Universidad Nacional de La Plata, Calle 64 y diagonal 113, 1900 La Plata, Argentina

ARTICLE INFO

Article history:

Received 21 November 2013

Received in revised form 7 April 2014

Accepted 13 May 2014

Available online 27 May 2014

Keywords:

N-nitrosodimethylamine (NDMA)

Dimethylamine (DMA)

Hydrogen

Ni{1 1 1} surface

Coadsorption

Dissociation

First principles calculations

ABSTRACT

N-nitrosodimethylamine (NDMA) reaction with coadsorbed hydrogen on the Ni{1 1 1} surface has been investigated in the low coverage regime using first-principles calculations. The results of previous calculations found that isolated NDMA adsorbs on the Ni surface in two different competitive ways as the two most stable configurations. In the *upright* configuration the adsorption is via the ON end. This configuration is slightly preferred energetically to the *flat* configuration, in which the interaction is via the ONN plane. However, this last configuration leads to a facile dissociation of the NDMA molecule via the N–N bond. In the present article, it is found that the formation of dimethylamine (DMA) and NO on the surface is preferred to the formation of other products on the surface from the *flat* configuration in the low NDMA coverage regime. Hydrogen is needed for the DMA formation. Besides that, high coverage of adsorbed hydrogen decreases the activation energy needed to break the N–N bond in the *flat* adsorption configuration.

© 2014 Elsevier B.V. All rights reserved.

1. Introduction

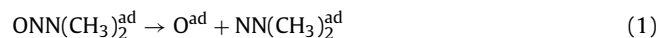
Many of the N-nitrosamine compounds attracted attention because of their carcinogenic power and other effects such as diabetes and foetal malformations. Since 1930 it has been reported that N-nitrosamines induce cancer to several small mammals and fish [1–3]. Although no direct link between human cancer and the exposure to N-nitrosamines has been established, it is suspected that this is the case [4].

It is well known that the formation of NDMA occurs in the process of water purification [5–12]. Traditional water treatment techniques (biodegradation, air stripping and activated carbon adsorption) are inefficient methods to degrade NDMA [13,14]. Two experimental techniques seem to be promising treatments for NDMA elimination from drinking water and waste-water: hydrogen-based membrane biofilm reactor (MBfR) [15] and catalysis [14,16–19]. The theoretical efforts of the present article are focused on this last method.

Experimental works have reported NDMA degradation on different metal catalysts (in the presence of hydrogen or in its absence) [14,16–19]. Most of the results show nickel as key element in the catalysts. Nickel seems to be a very active component in

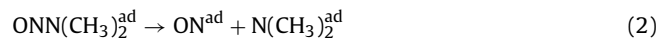
the catalysis process even in very small concentrations. Different mechanisms have been proposed for NDMA ($\text{ONN}(\text{CH}_3)_2$) decomposition under different conditions on metal catalysts [14,16–19]. Two mechanisms for NDMA decomposition on metal surfaces were described in a previous article [20] and they are summarized here:

1. initial N–O bond cleavage of the adsorbed NDMA molecule



to form ammonia (NH_3) and dimethylamine ($\text{HN}(\text{CH}_3)_2$, DMA), after interaction with hydrogen in several steps.

2. initial N–N bond cleavage of the adsorbed NDMA molecule



to form dimethylamine ($\text{HN}(\text{CH}_3)_2$) and ammonia (NH_3) or dinitrogen (N_2), after interaction with hydrogen.

Two stable adsorption configurations were reported as the most stable for NDMA on the Ni{1 1 1} surface: *upright* and *flat* [20]. In the *upright* configuration the NDMA molecule is bound to the surface via the ON end to two different atoms of the surface. NDMA dissociation from this configuration is described by Eq. (1). On the other hand, in the *flat* adsorption configuration the NDMA molecule is bound to the surface via the ONN plane to three different nickel atoms. NDMA dissociation from this adsorption configuration is

E-mail address: vranea@inifta.unlp.edu.ar



described by Eq. (2). It was also shown, in that article [20], that breaking the N–O (Eq. 1) or N–N (Eq. 2) bonds are favorable processes on the Ni{111} surface. However, the activation energy needed to cleave the N–N bond (Eq. 2) is lower by 0.33 eV than that one needed to break the N–O bond (Eq. 1). This indicates that NDMA fragmentation via the N–N bond cleavage (Eq. 2) seems to be more likely.

In this article, the coadsorption of NDMA adsorbed in the *flat* configuration with low hydrogen coverage on the Ni{111} surface and the final formation of fragments on the surface are investigated. Low coverage of NDMA is assumed. In this configuration the adsorption takes three metal atoms of the surface. Otherwise, at a higher coverage the *upright* configuration will probably dominate the adsorption. Several adsorption *hollow* sites are studied for H near adsorbed NDMA. Only the hydrogen that adsorbs on the surface is taken into account in this manuscript. The interactions between NDMA and hydrogen described here occur in aqueous environment and the mentioned species could interact not only via the surface but via other mechanisms. Interaction (repulsion) energies are calculated between adsorbates. After that initial interaction two dissociation pathways are investigated:

1. NO and DMA formation



2. HNO and N(CH₃)₂ formation



The results presented here show that although both interaction pathways (Eqs. (3) and (4)) are favorable energetically, NO and DMA formation is more likely to occur (Eq. (3)) from the *flat* configuration at low NDMA coverage. The effect of coadsorbed hydrogen on the energy barrier for NDMA dissociation is also investigated.

2. Methodology

First-principles total energy calculations were performed using density functional theory (DFT) as implemented in the Vienna Ab initio Simulation Package (VASP) [21,22]. The Kohn–Sham equations were solved using the projector augmented wave (PAW) approach for describing electronic core states [23,24] and a plane-wave basis set including plane waves up to 400 eV. Electron exchange and correlation energies were calculated within the generalized gradient approximation (GGA) in the Perdew–Wang 91 form [25]. Spin-polarization calculations have been performed for isolated adsorbed and coadsorbed NDMA molecule. Atomic relaxations are considered converged when the forces on the ions are less than 0.03 eV/Å. The climbing image nudged elastic band method (CI-NEB) was used to calculate the activation energies. Only one image was used that was forced to the maximum in the potential energy path between the initial and final stable configurations. In a previous article [20] the CI-NEB method was used to calculate the minimum energy path (MEP) of the isolated adsorbed NDMA molecule using five images. Only one maximum was found and the activation energy for fragmentation was calculated (0.23 eV). In the present report only one image is used in order to calculate or estimate only the activation energy for NDMA fragmentation.

The system (the Ni{111} surface and the adsorbate(s)) was modeled by a hexagonal supercell with lattice constants $a = 7.471$ and $c = 20.334\text{ \AA}$ [26]. The surface was modeled by 4-layer thick slab separated by more than 15 Å vacuum region to avoid interactions between slabs due to periodic boundary conditions. A (3×3) surface was used to minimize lateral interactions. The atoms of the two external layers and the adsorbate were allowed to freely relax

according to the calculated forces on them. The first Brillouin zone of the supercell was sampled with a $(4 \times 4 \times 1)$ Γ centered mesh, that gives 10 automatic \mathbf{k} -points. This is the only difference in the computational configuration with respect to the previous report [20].

The adsorption energy, E , was calculated as:

$$E = \text{TE} \left(\frac{\text{adsorbate}}{\text{srf}} \right) - \sum_j \text{TE}_j(\text{adsorbate}) - \text{TE}(\text{srf})$$

the *adsorbate* refers to the adsorbed species. The first term is the energy of the optimized configuration of adsorbed species on the clean relaxed surface. The second term is the gas phase energy of the adsorbate, half of the molecular H_2 energy is used for atomic hydrogen. The third term is the energy of the clean optimized Ni surface. With this definition, negative values of E stand for stable configurations.

3. Results and discussion

In a previous article [20], two stable adsorption configurations were found as the most stable for NDMA on the Ni{111} surface: *upright* and *flat*. The NDMA molecule binds via the ON end to two nickel atoms of the surface in the *upright* configuration, as shown in the left panel of Fig. 1. In the *flat* configuration, the NDMA molecule binds to three atoms of the surface via its ONN plane, as shown in the central and right panels of Fig. 1. In that article [20] and in the present manuscript, van der Waals (vdW) interactions are not included. If they were included, probably the interactions between the NDMA molecule and the nickel surface would be a bit stronger, mainly in the *flat* adsorption configuration. This means that the calculated adsorption energy would be a bit higher in absolute value. However, the adsorption would not change, probably [27]. The adsorption would still be via the oxygen and nitrogen atoms to three nickel atoms of the surface. The ONN plane would still be nearly parallel to the surface plane, although probably at a different distance [28]. The adsorption of a larger molecule, but still planar, has been studied with and without vdW interactions on the Ag{111} surface [28]. The calculated adsorption energy of azobenzene is 0.1 eV using PBE but 0.98 eV using vdW-DF [28]. This last value is in agreement with the experimental desorption energy, 1.0 ± 0.1 eV [29]. For NDMA adsorption on the Ni{111} surface in the *flat* configuration is not expected such a large value for the vdW forces. In fact, on the same surface used in the present manuscript, Ni{111}, the vdW interactions seem not to be present when adsorption of phenol is investigated using PBE ([30] and references within [31]).

In that article [20], the activation energy needed to dissociate the NDMA molecule into two fragments was calculated. From the *upright* configuration the cleavage of the O–N bond leaves O and NN(CH₃)₂ adsorbed on the surface (Eq. (1)). The cleavage of the N–N bond from the *flat* configuration produces NO and N(CH₃)₂ adsorbed on the surface (Eq. (2)). The *upright* adsorption configuration is favorable to the *flat* configuration by 0.13 eV. However, the activation barrier to dissociate NDMA from the *flat* configuration into NO and N(CH₃)₂ is lower by 0.33 eV. Although the NDMA adsorption in the *flat* configuration is less likely than the adsorption in the *upright* configuration, the NDMA dissociation from the *flat* configuration is much more likely. In order for the NDMA molecule to adsorb in the *flat* configuration low coverage is required, otherwise, the *upright* configuration is going to dominate. In the present report, the coadsorption of H and NDMA in the *flat* configuration, the N–N bond fragmentation and the formation of products are investigated.

Calculated adsorption energy for NDMA in the *flat* configuration is -0.82 eV. The ON, NN, NC and CH calculated bond lengths

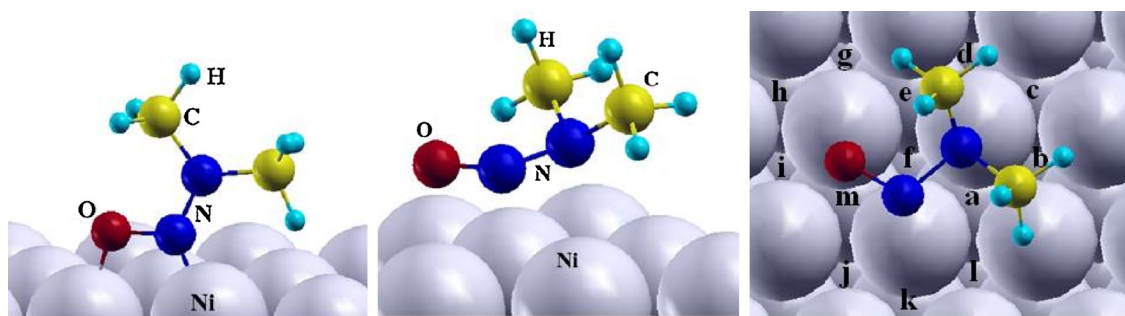


Fig. 1. (Left panel) Balls model for the NDMA adsorption in the *upright* configuration. (Central and right panels) Balls model for NDMA adsorbed in the *flat* configuration (lateral and top view, respectively). On the panel on the right, the letters mark the different H coadsorption configurations investigated. Table 1 and Fig. 2 show the calculated repulsion and adsorption energies for every coadsorption configuration. Big and small light (light blue) balls stand for Ni and H atoms, respectively. Black (blue), dark (red) and light (yellow) medium balls stand for N, O and C atoms, respectively. (For interpretation of the references to color in this figure legend, the reader is referred to the web version of the article.)

are 1.32, 1.51, 1.48 and 1.10 Å, respectively; the ONN bond angle is 109.6°. These values are compared with those calculated for the isolated NDMA molecule: 1.24, 1.35, 1.45 and 1.10 Å, for the ON, NN, NC and CH bond lengths, respectively; the calculated ONN bond angle is 115.8°. As can be seen, the O—N—N part of the NDMA molecule is the most affected by the interaction with the surface. The optimized O—Ni and N—Ni bond lengths are 1.95, 1.93 and 2.04 Å, respectively.

Calculated adsorption energies for isolated atomic hydrogen on the Ni{111} surface are −0.59 and −0.57 eV for *fcc* and *hcp hollow* sites, respectively. The H—Ni bond lengths are 1.70 Å in both adsorption configurations.

In order to investigate the interaction between adsorbed species, hydrogen is adsorbed on the neighbor *hollow* sites around the NDMA molecule in the *flat* configuration. Only coadsorbed

hydrogen is taken into account. The right panel of Fig. 1 shows a schematic top view of the different investigated H and NDMA coadsorption configurations.

Hydrogen and NDMA coadsorption is stable in all marked configurations in Fig. 1 except in the *fcc hollow* site marked with *i*. Fig. 2 shows the energy diagram of H coadsorption and reaction with NDMA on the Ni{111} surface. Half of the calculated energy of molecular hydrogen, the energy of the isolated NDMA and the energy of the clean optimized Ni{111} surface are taken as the reference energy (stage A in Fig. 1). Adsorbed NDMA without interaction with adsorbed H is stable with respect to that energy of reference (the systems H/Ni{111} and NDMA/Ni{111} are separated by an infinite distance, stage B). The energy of non-interacting adsorbed H and adsorbed NDMA is calculated as

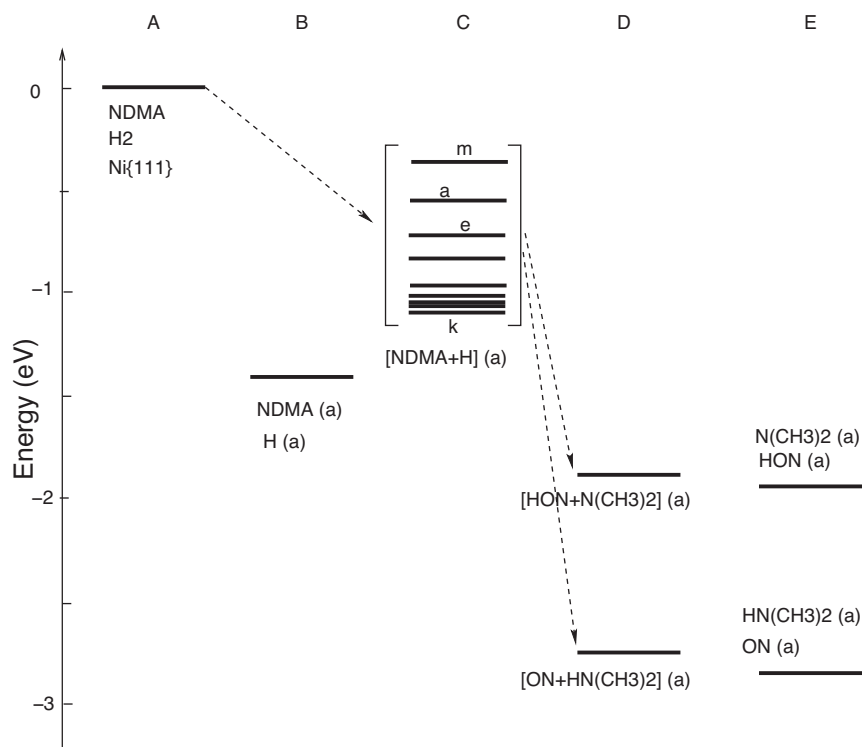


Fig. 2. Energy diagram for NDMA dissociation assisted by coadsorbed hydrogen. Stage A: energy of reference: NDMA gas phase energy, half of the H₂ gas phase energy and clean optimized Ni{111} energy. Stage B: isolated NDMA adsorption and isolated H adsorption separated by an infinite distance ($E_{\text{non}} \approx -1.40$ eV). Stage C: adsorption energy, E_a , of NDMA and H. The most unstable adsorption configurations are (from the top) configurations *m*, *a* and *e*. The most stable adsorption configuration is *k* (see Fig. 1 and Table 1). Stage D: two possible pathways for NDMA dissociation across the N—N bond: HON—N(CH₃)₂ or ON—HN(CH₃)₂ coadsorption. Stage E: adsorption of the species separated at infinite distance.

Table 1

Adsorption and repulsion energies (E and E_r in eV) in the H-NDMA coadsorption configurations. Different H adsorption on *hollow* sites around the NDMA molecule adsorbed in the *flat* configuration. The letters individualize H adsorption sites shown in Fig. 1 right panel. Hydrogen subsurface adsorption in configuration *f*. Configuration *i* is not stable. Also shown, in the bottom part, the H-NDMA distances and the H–Ni bond lengths (in Å) for the *m*, *a* and *e* configurations (configurations where coadsorbates adsorb on two common surface atoms). Isolated H–Ni bond lengths are 1.70 Å.

H ads site	<i>m</i>	<i>a</i>	<i>e</i>	<i>b</i>	<i>l</i>	<i>c</i>	<i>h</i>	<i>d</i>	<i>j</i>	<i>g</i>	<i>k</i>	<i>f</i> (ss)
E	−0.29	−0.51	−0.84	−0.93	−1.06	−1.07	−1.07	−1.09	−1.09	−1.11	−1.14	−0.69
E_r	1.11	0.88	0.55	0.49	0.35	0.32	0.32	0.31	0.31	0.30	0.25	
H–NDMA distances	2.13	2.18	2.32									
H–Ni	2.19	2.22	2.39									
Bond Lengths	1.66	1.71	1.71									
	1.57	1.61	1.67									
	1.51	1.52	1.57									

$E_{\text{non}} = E^{\text{H}} + E^{\text{NDMA}} = -0.59 \text{ eV} + (-0.82 \text{ eV}) = -1.41 \text{ eV}$ as long as the H adsorption is on the *fcc hollow* site and -1.39 eV when H adsorption takes place on *hcp hollow* site (stage *B*) (Fig. 3).

From stage *A*, NDMA and H adsorption takes place on the nickel surface in some of the configurations shown on the right panel of Fig. 1. Assuming the same coverage of H and NDMA, the adsorption energy will be one of the energies shown in stage *C* in Fig. 2. All the values of the adsorption energy are between -1.14 and -0.29 eV . The difference between the calculated adsorption energy E (stage *C* in Fig. 2) and the energy of non-interacting adsorbed H and NDMA, E_{non} (stage *B*), is the interaction energy between the two adsorbates, E_r . Positive values of E_r indicate repulsive interaction.

Table 1 reports that the calculated repulsive interaction energy, E_r , between adsorbates is maximum in the configurations in which the H is adsorbed in the position marked as *m*, *a* and *e* in Fig. 1 ($E_r = 1.11$, 0.88 and 0.55 eV , respectively). This indicates that the configurations in which the hydrogen is adsorbed on the *hollow* sites marked as *m*, *a* and *e*, with respect to the NDMA adsorbed in the *flat* configuration, are the less likely of all the stable configurations marked in Fig. 1. At low hydrogen coverage, configurations with less repulsive energy are the most likely. When the hydrogen coverage increases, configurations with higher repulsive energies are more likely than at lower coverage. High hydrogen coverage is required in order to increase the probabilities of configurations *m*, *a* and *e*. The configurations where the H atom adsorbs on the sites *m*, *a* and *e* respect to the NDMA molecule adsorbed in the *flat* configuration are the only three configurations where both adsorbates are bound to two common surface nickel atoms.

A comparison of the distances between the coadsorbed hydrogen atom and the NDMA molecule, in these three coadsorption configurations, shows that for slightly longer distances the repulsion between adsorbates is smaller (bottom part of the Table 1). The distances between the coadsorbed hydrogen and the two nearest NDMA atoms are shorter in the *m* configuration. As a consequence, the repulsion is stronger than in the *a* and *e* configurations where the distances are longer.

In the *f* configuration the hydrogen adsorption is subsurface, there is not a stable configuration in which the hydrogen atom is adsorbed on the surface.

H-NDMA repulsive energy is lower in configurations in which the adsorbates are bound to one common nickel atom. Most of these repulsion energies are in the range 0.30 – 0.35 eV . The configurations with the lowest adsorption energy (absolute value), due to the highest repulsion energy (H in positions *m*, *a* or *e*), are less likely to occur than the other coadsorption configurations and probably high hydrogen coverage is required in order for the hydrogen to occupy some of these sites. For low hydrogen coverage configurations in which the repulsive energy is lower are going to happen first, probably. For higher coverage, configurations in which the repulsive energy is higher are going to happen. This is, for low hydrogen coverage, the hydrogen atom is going to adsorb first in the site *k*. As

the hydrogen coverage increases the hydrogen atoms are going to fill, probably, the sites *g*, *j*, *d*, *h*, *c*, *l*, *b*, *e*, *a* and *m*.

In a previous article [20], the energy barrier needed to dissociate the adsorbed NDMA molecule across the N–N bond from the *flat* configuration was calculated in about 0.23 eV . It was found, in that article [20], that the ON and $\text{N}(\text{CH}_3)_2$ fragments have a stable adsorption on top of, or monocoordinated to, one nickel atom of the surface. The top three panels in Fig. 4 show a balls model for the initial isolated NDMA adsorption in the *flat* configuration, the maximum in the PES and the final $\text{NO}-\text{N}(\text{CH}_3)_2$ coadsorption, from left to right, respectively. The first line in Table 2 shows the N–N bond in the initial state (isolated NDMA adsorption) is 1.51 \AA (see upper row, left panel of Fig. 4), to finally reach a N–N distance of almost 2 \AA (see upper row, right panel of Fig. 4). In the maximum of the PES the N–N distance is 1.64 \AA (see upper row, central panel in Fig. 4).

How does hydrogen coadsorption on different sites shown in Fig. 1 affect the energy barrier needed to dissociate the adsorbed NDMA via the N–N bond?

Calculated energy barriers for H-NDMA coadsorption configurations where the hydrogen is adsorbed on the sites *b*, *c* and *d* are in the range 0.21 – 0.23 eV . These adsorption configurations are among the most likely to occur because of the low repulsive energy between the adsorbed species, as Table 1 indicates. Hydrogen coadsorption in the mentioned configurations does not decrease strongly the activation energy for isolated NDMA dissociation on the surface. Hydrogen adsorption on the site marked as *f* does not decrease markedly the activation energy for NDMA dissociation (from 0.23 eV to 0.19 eV).

The hydrogen coadsorption on the sites marked as *a* and *e* in Fig. 1 is unlikely for low hydrogen coverage due to a higher repulsive energy, as Table 1 indicates. However, the energy barrier for NDMA dissociation is decreased to $\approx 0.07 \text{ eV}$ (from 0.23 eV) once hydrogen adsorption takes place. This energy is almost the energy difference between initial and final states. These results predict that the hydrogen coadsorption on the sites marked with *a* and *e* in Fig. 1 increase significantly the probabilities of NDMA dissociation on the $\text{Ni}\{111\}$ surface.

It should be noticed from Table 2 that N–N bond length of the NDMA molecule is not strongly modified by H coadsorption on sites *a* or *e* (1.53 and 1.49 \AA , respectively). However, for hydrogen coadsorption on site *a* in the maximum of the PES, the N–N

Table 2

Distances in the isolated NDMA adsorption and in the *a* and *e* coadsorption configurations (see Fig. 4): nitrogen–nitrogen and nitrogen–hydrogen distances.

	Initial		Maximum		Final	
	N–N	N–H	N–N	N–H	N–N	N–H
Isolated	1.51		1.64		1.98	
<i>a</i>	1.53	2.24 2.21	2.07	2.25 2.21	2.09	2.23 2.20
<i>e</i>	1.49	2.69 2.37	1.74	2.90 2.47	1.93	3.09 2.45

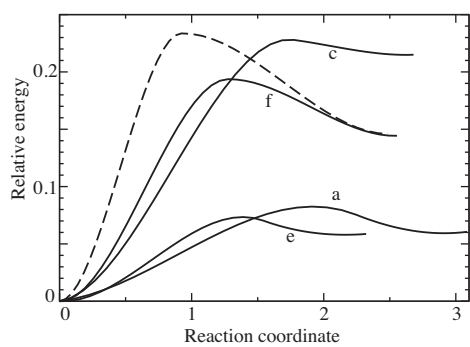


Fig. 3. Dissociation of the NDMA molecule adsorbed in the *flat* configuration. Relative energy (eV) vs reaction coordinate (\AA). On the left, the relative energy of the adsorbed NDMA molecule, with or without a coadsorbed H atom. Dashed line stands for the fragmentation of the isolated NDMA adsorbed on the Ni{111} surface. The activation energy for NDMA dissociation to ON and $\text{N}(\text{CH}_3)_2$ fragments (right side) is around 0.23 eV. Solid lines marked with the letters stand for NDMA fragmentation after H adsorption on the sites marked in Fig. 1.

distance is longer by 0.43 \AA than in the isolated NDMA adsorption, whereas it is only 0.1 \AA longer when hydrogen adsorption is on site *e*. A comparison of the final states shows that the N–N distance is longer by 0.11 \AA when adsorption takes place on site *a* and shorter by 0.05 \AA than the isolated NDMA adsorption. Also, the coadsorbed H–N distances in this configuration are not mostly affected upon NDMA adsorption. They are about 2.2 \AA no matter the NDMA adsorption is molecular or after NDMA dissociation.

A comparison between the states labeled as *maximum* and *final* for hydrogen coadsorption on sites *a* and *e*, shows the structures of the *maximum* and the *final* states are very similar. Also, the energy difference, 0.01 eV, is very small, in both cases. It seems that in these cases, *a* and *e*, the *final* state is wide and includes the *maximum* found in the calculations (within the error of the calculations). And so, the activation energy for NDMA dissociation seems to be the energy difference between the *initial* and the *final* states.

Isolated NDMA dissociation on the Ni{111} surface is produced with an activation energy of 0.23 eV. For low coverage of H, only sites with low repulsive energy are going to be filled, site *c*, for example. It is unlikely that sites such as *a* or *e* will be filled at low H coverage. Under these conditions the coadsorption of H does not decrease that activation energy and the adsorbed H species only help in the formation of the DMA molecule only after the NDMA molecule dissociates on the surface. If the H coverage is higher, sites *a* and *e* are going to be filled and the activation barrier for NDMA dissociation is going to be lower, increasing the probabilities of dissociation. In order to increase the probabilities of NDMA dissociation, adsorbed in the *flat* configuration, high hydrogen coverage is required to increase the probabilities of hydrogen adsorption on sites *a* and *e*.

After NDMA and H coadsorption and after NDMA dissociation breaking the N–N bond on the Ni{111} surface (stage C shown in Fig. 2) two pathways are investigated: the H atom could bind to the NO fragment or to the $\text{N}(\text{CH}_3)_2$ fragment.

Stage *D* in Fig. 2 shows both pathways are stable and more likely than any of the stable H–NDMA coadsorption configurations.

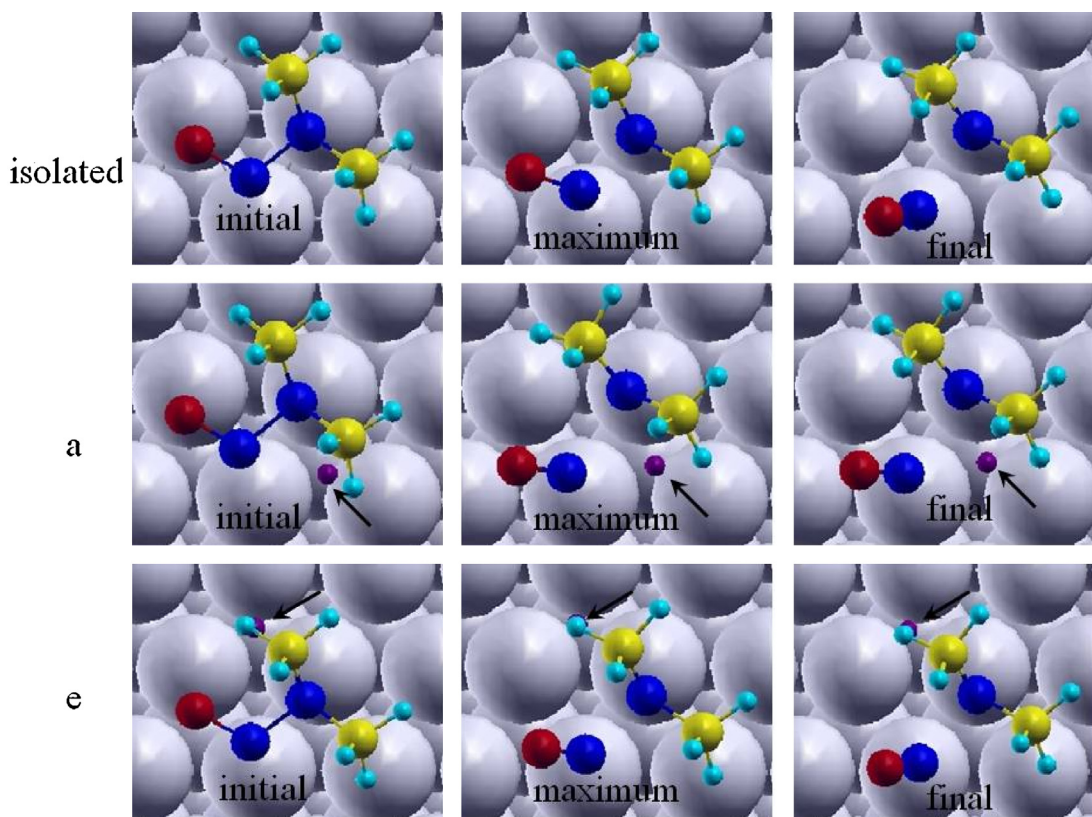


Fig. 4. Balls model for NDMA dissociation to NO and $\text{N}(\text{CH}_3)_2$ on the intermediate configuration on the Ni{111} surface (see reference [20]). The three top panels show top views of the isolated NDMA adsorption, the maximum in the MEP and dissociated NDMA (from left to right). The central and bottom three panels show top views of the NDMA + H coadsorption in the configurations *a* and *e* (respectively), from left to right, NDMA molecular coadsorption, the maximum in the MEP and final fragments, NO– $\text{N}(\text{CH}_3)_2$ –H. See right panel of Fig. 1. The N–N and N–H distances are shown in Table 2. Big light (light blue) balls stand for Ni atoms. Black (blue), dark (red) and light (yellow) medium balls stand for N, O and C atoms, respectively. Light (light blue) and dark (purple) small balls stand for the CH_3 hydrogens and the coadsorbed H, respectively. The arrow indicates position of the coadsorbed H. (For interpretation of the references to color in this figure legend, the reader is referred to the web version of the article.)

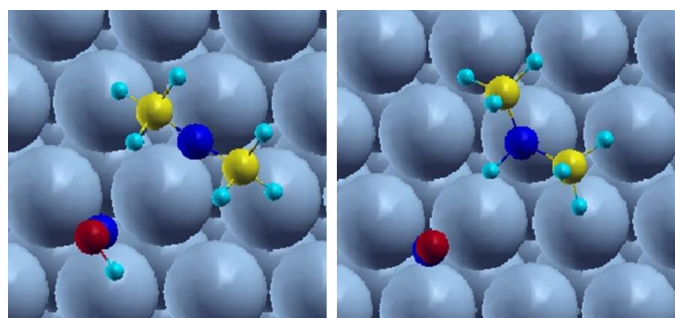


Fig. 5. Balls model for the coadsorption of the fragments after N–N cleavage. On the left, the NOH and $\text{N}(\text{CH}_3)_2$ fragments. On the panel on the right, NO and DMA fragments where the N–H bond is in the direction of the NO fragment. The corresponding energies are included in the Stage D in Fig. 2. Big and small light blue balls stand for Ni and H atoms, medium blue, red and yellow balls stand for N, O and C atoms, respectively. (For interpretation of the references to color in this figure legend, the reader is referred to the web version of the article.)

Formation of the NOH and $\text{N}(\text{CH}_3)_2$ fragments adsorbed on the Ni surface is stable by -1.83 eV , whereas if the hydrogen atom binds to the $\text{N}(\text{CH}_3)_2$ fragment in order to form NO and DMA adsorbed on the Ni surface, the adsorption energy is -2.87 eV . Comparison of these two energies indicates that formation of NO and DMA ($\text{HN}(\text{CH}_3)_2$) is more stable by more than 1 eV on this nickel face and much more likely to occur. Fig. 5 shows a balls model for the optimal configuration found in which the H is bound to the oxygen of the NO end. The repulsion energy between fragments is about 0.03 eV , as stage E shows. Hydrogen bound to the nitrogen of the NO fragment is not stable.

The other pathway shown in Fig. 2 stage D, from H and NDMA co-adsorption, shows a more favorable N–N bond fragmentation. Production of NO and DMA co-adsorbed on the surface is exothermic by 2.87 eV , as long as the N–H bond is in the direction of the NO fragment. This value is 1.04 eV energetically favorable against $\text{NOH}-\text{N}(\text{CH}_3)_2$ formation on the nickel surface.

DMA and N_2 molecules have been found in recent experiments [14]. NDMA and H_2 have been co-adsorbed on Raney catalysts in aqueous environment. In the experiments, the authors report DMA production simultaneously with the NDMA elimination. Final amount of DMA is reported equal to the initial NDMA amount as an indication that each NDMA molecule produces one DMA molecule. The same experimental results show a delay in the N_2 production and the final measurement is about half of the initial NDMA amount. This result could mean that two NDMA molecules are needed to produce one N_2 molecule. The N_2 formation from two NO molecules on the surface and posterior desorption needs a few intermediate steps to be completed. Probably, all the intermediate steps are activated processes and this could explain the delay in the N_2 formation as experimental results show.

4. Conclusions

In a previous article, two stable NDMA adsorption configurations on $\text{Ni}\{1\ 1\ 1\}$ were found: *upright* and *flat*. Dissociation from the *flat* configuration is more likely due to a lower activation energy to break the N–N bond into NO and $\text{N}(\text{CH}_3)_2$ fragments. In the present report the effect of the coadsorption of atomic hydrogen with NDMA in the *flat* adsorption configuration is investigated. Although coadsorption is stable for the investigated configurations, a repulsion energy between 0.25 and 1.11 eV is calculated between H and NDMA in all these configurations.

The H coadsorption around the NDMA molecule adsorbed in the *flat* configuration has different effects on the activation energy

for its dissociation. The activation energy for NDMA dissociation is notably reduced from 0.23 to 0.07 eV when H adsorption takes place in the sites marked with the letters *a* and *e* in Fig. 1. The last value is almost the energy difference between the initial and final stable states. Together with the fact that the maximum and the final states are very similar indicate that probably the final state is wide and it is the maximum in the PES.

In these two adsorption configurations, both adsorbates are bound to two common nickel atoms. Also, in these configurations the H fragment is around the N–N bond in a way in which makes the formation of the more stable DMA configuration easy with its NH bond near the NO fragment. The adsorption energies of the configurations *a* and *e* are smaller than most of the other configurations and the probabilities of occupancy are also lower. In order to populate these sites, high H coverage is needed.

After NDMA dissociation, two pathways for H reaction with the fragments are studied: formation of HNO and $\text{N}(\text{CH}_3)_2$ and formation of NO and DMA ($\text{HN}(\text{CH}_3)_2$); the last one being more stable by more than 1 eV . These theoretical results support the experimental results [14]. They show DMA formation from H and NDMA in aqueous media. Also, the final amount of DMA is about the same as the initial NDMA. This is also in agreement with the model exposed here that shows formation of one DMA molecule from each initial NDMA molecule. Experimental results [14] also show that the formation of N_2 is about half of the initial amount of NDMA. In the model introduced in this report, N_2 formation is from two NO fragments and each fragment is formed after dissociation of one NDMA molecule.

Acknowledgments

This work has been supported by Consejo de Investigaciones Científicas y Técnicas (CONICET), Argentina. Thanks to Prof. W.F. Schneider, T.J. Strathmann and J.R. Shapley for initial talks on this subject.

References

- [1] H.A. Freund, Ann. Intern. Med. 10 (1937) 1144.
- [2] J.M. Barnes, P.N. Magee, Brit. J. Ind. Med. 11 (1954) 167.
- [3] P.N. Magee, J.M. Barnes, Brit. J. Cancer 10 (1956) 114.
- [4] S. Patai (Ed.), The chemistry of amino, nitroso and nitro compounds and their derivatives. Part 2, John Wiley and Sons, 1982.
- [5] W.A. Mitch, A.C. Gerecke, D.L. Sedlak, Water Res. 37 (2003) 3733–3741.
- [6] W.A. Mitch, D.L. Sedlak, Environ. Sci. Technol. 37 (2004) 1445–1454.
- [7] W.A. Mitch, D.L. Sedlak, Environ. Sci. Technol. 36 (2002) 588–595.
- [8] J. Choi, R.L. Valentine, Water Res. 36 (2002) 817–824.
- [9] J. Choi, S.E. Durk, R.L. Valentine, J. Environ. Monit. 4 (2002) 249–252.
- [10] E. Pehlivanoglu-Mantas, D.L. Sedlak, Water Res. 40 (2006) 1287–1293.
- [11] E. Pehlivanoglu-Mantas, A.L. Hawley, R.A. Deeb, D.L. Sedlak, Water Research 40 (2006) 341–347.
- [12] I.M. Schreiber, W.A. Mitch, Environ. Sci. Technol. 39 (2005) 3811–3818.
- [13] C. Lee, J. Yoon, U. Von Gunten, Water Research 41 (2007) 581–590.
- [14] A.J. Friedich, J.R. Shapley, T.J. Stathmann, Environ. Sci. Technol. 42 (2008) 262–269.
- [15] J. Chung, G.-H. Ahn, Z. Chen, B.E. Rittmann, Chemosphere 70 (2008) 516–520.
- [16] M.G. Davie, M. Reinhard, J.R. Shapley, Environ. Sci. Technol. 40 (2006) 7329–7335.
- [17] L. Gui, R.W. Gillham, M.S. Odziemkowski, Environ. Sci. Technol. 34 (2000) 3489–3494.
- [18] M.S. Odziemkowski, L. Gui, R.W. Gillham, Environ. Sci. Technol. 34 (2000) 3495–3500.
- [19] C.H. Schaefer, C. Topoleski, M.E. Fuller, Water Environ. Res. 79 (2007) 57–62.
- [20] V.A. Ranea, T.J. Strathmann, J.R. Shapley, C.J. Werth, W.F. Schneider, Chem-CatChem 3 (2011) 1–7.
- [21] G. Kresse, J. Hafner, Phys. Rev. B 49 (1994) 14251.
- [22] G. Kresse, J. Furthmüller, Phys. Rev. B 54 (1996) 11169–11186.
- [23] P. Blöchl, Phys. Rev. B 50 (1994) 17953.
- [24] G. Kresse, J. Joubert, Phys. Rev. B 59 (1999) 1758.

- [25] J.P. Perdew, J.A. Chevary, S.H. Vosko, K.A. Jackson, M.R. Pederson, D.J. Singh, C. Fiolhais, Phys. Rev. B 46 (1992) 6671–6687.
- [26] R.W.G. Wyckoff, Crystal Structures, second ed., Interscience, New York, 1965.
- [27] J. Carrasco, J. Klimes, A. Michaelides, J. Chem. Phys. 138 (2013) 024708.
- [28] G. Li, I. Tamblyn, V.R. Cooper, H-J. Gao, J.B. Neaton, Phys. Rev. B 85 (2012) 121409.
- [29] G. Mercurio, et al., Phys. Rev. Lett. 104 (2010) 036102.
- [30] D.C. Langreth, B.I. Lundqvist, S.D. Chakarova-Käck, V.R. Cooper, M. Dion, P. Hyldgaard, A. Kelkkanen, J. Kleis, coworkers, J. Phys.: Condens. Matter 21 (2009) 084203.
- [31] L. Delle Site, A. Alavi, A.F. Abrams, Phys. Rev. B 67 (2003) 193406.